NEURO-ONCOLOGY

Survival analysis for apparent diffusion coefficient measures in children with embryonal brain tumours

Matthew Grech-Sollars, Dawn E. Saunders, Kim P. Phipps, Jonathan D. Clayden, and Chris A. Clark

Imaging and Biophysics Unit, UCL Institute of Child Health, University College London (M.G.-S., J.D.C., C.A.C.); Departments of Radiology (D.E.S.) and Department of Neuro-oncology (K.P.P.), Great Ormond Street Hospital for Children, London, United Kingdom

Embryonal brain tumors constitute a large and important subgroup of pediatric brain tumors. Apparent diffusion coefficient (ADC) measures have been previously used in the analysis of these tumors. We investigated a newly described ADC-derived parameter, the apparent transient coefficient in tumor (ATCT), a measure of the gradient change of ADC from the peri-tumoral edema into the tumor core, to study whether ATCT correlates with survival outcome. Sixty-one patients with histologically proven embryonal brain tumors and who had diffusion-weighted imaging (DWI) as part of their clinical imaging were enrolled in a retrospective study correlating ADC measures with survival. Kaplan-Meier survival curves were constructed for extent of surgical resection, age <3 years at diagnosis, tumor type, and metastasis at presentation. A multivariate survival analysis was performed that took into consideration ATCT and variables found to be significant in the Kaplan-Meier analysis as covariates. Results from the multivariate analysis showed that ATCT was the only significant covariate ($P < .001$). Survival analysis using Kaplan-Meier curves, dividing the patients into 4 groups of increasing values of ATCT, showed that more negative values of ATCT were significantly associated with a poorer prognosis ($P < .001$). A statistically significant difference was observed for survival data with respect to the change in ADC from edema into the tumor volume. Results show that more negative ATCT values are significantly associated with a poorer survival among children with embryonal brain tumors, irrespective of tumor type, extent of resection, age <3 years at diagnosis, and metastasis at presentation.

Keywords: apparent transient coefficient, diffusion MRI, pediatric cancer, peri-tumoral edema, tumor border.

Embryonal brain tumors constitute a large and important subgroup of pediatric central nervous system (CNS) tumors and are a group of malignant tumours characterized by small round cells and high cellularity. They are classified into 3 main groups: medulloblastoma; supratentorial primitive neuroectodermal tumors (sPNET), also known as CNS-PNET; and atypical teratoid/rhabdoid tumours (ATRT).[1–4] Because of their common cellular features, they share similar characteristics when analyzed using diffusion-weighted imaging (DWI), a submodality of magnetic resonance imaging (MRI).

DWI and, more specifically, the apparent diffusion coefficient (ADC), are increasingly used in the diagnosis and treatment of various tumor types. ADC, a measure of the diffusion of water, has been found to be a good biomarker for inferring tumor cellularity.[5–8] Regions of increased cellularity provide barriers for diffusion, restricting water motion and thereby exhibiting a lower ADC. The ADC is also affected by intracellular space: a high nucleus to cytoplasm ratio limits the diffusion of water intracellularly and is thought to contribute to a reduction in ADC.[9,10] In areas where diffusion is not restricted, such as in cerebrospinal fluid (CSF), brain edema, and necrotic regions of the tumor, the ADC will have a higher value.

Noninvasive imaging biomarkers that aid in cancer treatment planning are of significant importance. Cancer imaging biomarkers based on DWI have been previously discussed from a clinical, neuroradiological,

and oncological perspective to review the current patho-physiological understanding of DWI.[11] MRI biomarkers examining the gradient change over the tumor borders have been previously studied.[12–14] One such biomarker is the apparent transient coefficient (ATC), which measures the gradient change in ADC at tumor borders.[13,14] Previous work examined the ATC from white matter into surrounding peri-tumoral edema (ATCO) and from the peri-tumoral edema into the tumor core (ATCT) and compared these with survival among adults with glioblastoma multiforme.[14] A correlation was found between ATCT and survival in that patient group; however, to our knowledge, no in-depth survival analysis was published.

The purpose of our research was to identify and analyze potential biomarkers that would predict survival outcome among children with embryonal brain tumors and aid in treatment planning and decision making. The work is based on the hypothesis that ATCT correlates with survival outcome in this important and highly malignant group of pediatric brain tumors. The tumors appear to be very dark on ADC images because of water restriction by both intra- and extracellular components.[9,10] We hypothesized that tumor cell density could be related to survival and examined a range of ADC measures for correlation with survival: minimum ADC, mean ADC, ATCT, and ATCO.

Materials and Methods

Patients

Sixty-one patients with histologically proven embryonal brain tumors and who had DWI as part of their clinical imaging from 2004 through 2011 were enrolled in a retrospective study to correlate ADC measures with survival. Three children with pineoblastomas (PNET of the pineal gland) were excluded from the study, because the lack of surrounding brain parenchyma and edema precludes measurement of ATCT. Thus, a total of 58 patients (31 male, 27 female; aged 3 weeks to 14.6 years; mean, 5.7 years) were analyzed. Ethical approval was given by the local research ethics committee. Informed consent was not required, because the data were obtained for clinical purposes. All data were anonymized in accordance with the data protection act.

Fifty-eight children were included: 44 with infratentorial and 14 with supratentorial tumors; 40 were medulloblastoma, 9 were ATRT (5 supratentorial and 4 infratentorial), and 9 were sPNET tumors.

Forty patients >3 years of age underwent surgery (31 had gross total surgical resection and 9 had partial surgical resection), and this was followed by radiotherapy and chemotherapy in 39 children. Of the remaining 18 patients <3 years of age at diagnosis, 14 underwent surgery (6 had gross total surgical resection and 8 had partial surgical resection); followed by both radiotherapy and chemotherapy in 5 children and chemotherapy alone in 9 children. Palliative care was given to 1 patient >3 years of age and 4 patients <3 years of age.

Imaging

Imaging data from 43 of the 58 patients were acquired on a 1.5T Siemens Magnetom Symphony MRI scanner, with a maximum magnetic field gradient strength of 30 mTm^{-1}. The data from the remaining 15 patients were acquired on a 1.5T Siemens Avanto scanner, with a maximum magnetic field gradient strength of 40 mTm^{-1}. DWI data were obtained using a diffusion-sensitized single-shot echo planar imaging sequence ($b = 0, 500, 1000 \text{ s mm}^{-2}$). Diffusion gradients were applied in 3 orthogonal directions, with an image matrix of 128×128 and field of view of 230×230 mm. On the Avanto scanner, 19 slices were acquired with a 5 mm thickness, 1.5 mm gap, and a total sequence time of 64 s, with TR = 2700 ms and TE = 96 ms. The Symphony protocol acquired 20 slices with a 5-mm thickness, 2.5-;mm gap, and a total sequence time of 56 s, with TR = 3600 ms and TE = 107 ms.

Measurements

Diagnostic clinical MRI scans obtained before gross total resection and any chemo- and radiotherapy treatment were used for data analysis. Minimum and mean ADC were included in the analysis and were calculated by applying a mask over the whole tumor, excluding peri-tumoral edema but including necrotic regions of the tumor, to include the extent of necrosis in the analysis. The size of necrotic area influenced the mean ADC, because of the higher ADC values in these areas.[15,16] Calculations for the minimum and mean ADC were performed using MATLAB (MathWorks).

The ATC, the gradient change in ADC over a series of voxels at the tumor border, was measured in 2 regions: white matter into surrounding peri-tumoural edema (ATCO) and peri-tumoural edema into the tumor core (ATCT). Gradients were calculated from ADC images visualized using FSLView (FMRIB Image Analysis Group) on the slice that contained the largest tumor area. The white matter–edema boundary and the edema-tumor boundary were identified on the selected image. Four consecutive voxels were selected, with the first voxel in white matter and the next 3 voxels in edema for the ATCO, and the first voxel in edema and the next 3 voxels in the tumor core for the ATCT (Fig. 1). A linear fit for these 4 points was applied to find the gradient change in ADC. Where possible, the gradient change in ADC was calculated at 4 different locations of the tumor, located by drawing a crosshair through the center of the tumor and averaged to determine the ATCO and ATCT used in the survival analysis. A width of 2 voxels was used, such that the ATCO and ATCT were averaged over 8 locations. It was expected that ATCO would be a positive gradient and ATCT would be a negative gradient, because ADC values in areas of edema are higher than both white matter and tumor areas. The ATC was not measured in necrotic regions of the tumor.
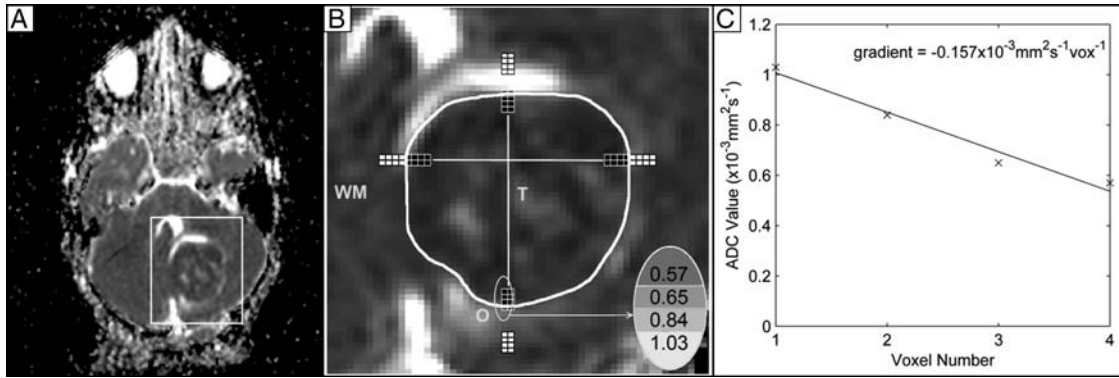
Fig. 1. Measuring the ATCT: the white box in (A) indicates the area on the ADC map that is analyzed. The edema-tumor boundary is identified as marked by the white contour in (B), which also shows the white matter (WM), peri-tumoral edema (O), and tumor core (T). The ATCT is measured at 4 different locations using a 2-voxel width as shown by the voxels highlighted in black. Therefore, ATCT is measured in a total of 8 locations. The calculation for the gradient change in ADC is shown in (C) and is performed by applying a linear fit to the circled ADC values for the vertical column of 4 pixels on the left, at the posterior side of the tumor. The gradient change in ADC is measured in all 8 locations, and the mean of these is the ATCT. In the image, voxels in white represent those voxels considered for measuring the ATCO.

Survival Analysis

A linear fit among survival and ATCO, ATCT, mean ADC, and minimum ADC was applied to analyze whether there was any significant linear correlation. R and P values were calculated for this linear correlation.

Kaplan-Meier survival curves[17] were plotted for age at diagnosis (<3 years or >3 years), extent of surgical resection (total or partial/none), tumor type (ATRT, medulloblastoma, or sPNET), and whether the patient had metastasis at presentation.

Parameters showing a significant difference from the Kaplan-Meier analysis and the linear fit were included in a multivariate survival analysis,[18] using a Cox proportional hazard regression model. The covariates considered were the ATCT, whether patients were aged <3 years at diagnosis, and the extent of surgery. To retain significant statistical power, a maximum of 3 covariates were included in the multivariate survival analysis, in compliance with suggestions outlined elsewhere.[19]

The ATCT was further analyzed by subdividing it into 4 groups of increasing ATCT values in such a way that an equal number of patients were included in each group and in accordance with the approach described elsewhere.[20] Kaplan-Meier survival curves were constructed to visualize the difference in survival among the 4 ATCT groups. Statistical analysis was performed using R software[21] and the survival analysis package therein.[22]

Reproducibility Study

An intra- and interobserver reproducibility study was conducted on the ATCT in a random selection of 10 patients. Measurements were taken after familiarization with the method, and intra-observer data were calculated from 2 measurements by an engineer with 3 years of medical imaging experience (M. G.-S.). Inter-observer analysis was performed between a set of measurements made by the same engineer and a second set made by a neuroradiologist with 10 years of neuroradiology experience (D. E. S.). The coefficient of variation was determined in these 10 patients for intra-observer and inter-observer agreement by using Bland-Altman analysis as proposed elsewhere.[23,24] Calculations were made, using the equations shown below, such that the coefficient of repeatability (CR) is defined as 1.96 times the standard deviation, and the coefficient of variance (COV) is given by CR divided by the mean of the observations and expressed as a percentage. The CR indicates the limits within which 95% of observations are expected to lie, with x_1 and x_2 being the first and second set of measurements taken, respectively.

$$CR = 1.96\sqrt{\frac{\sum (x_1 - x_2)^2}{n - 1}}$$

$$COV = \frac{CR}{\text{mean}(x_1, x_2)} \times 100\%$$

Results

Correlating ADC Measures with Survival

A plot of survival against ATCT (the gradient change in ADC from edema into the tumor) showed that those patients who died (21 of 58) had more negative ATCT values than did those who survived (Fig. 2A). The linear correlation between survival and ATCT was tested and showed a statistically significant correlation ($R = 0.49$, $P < .001$). It is clear from the plot that there is a wide range of survival, particularly as ATCT approaches zero; however, the data indicate a decreased chance of survival for highly negative values of ATCT.
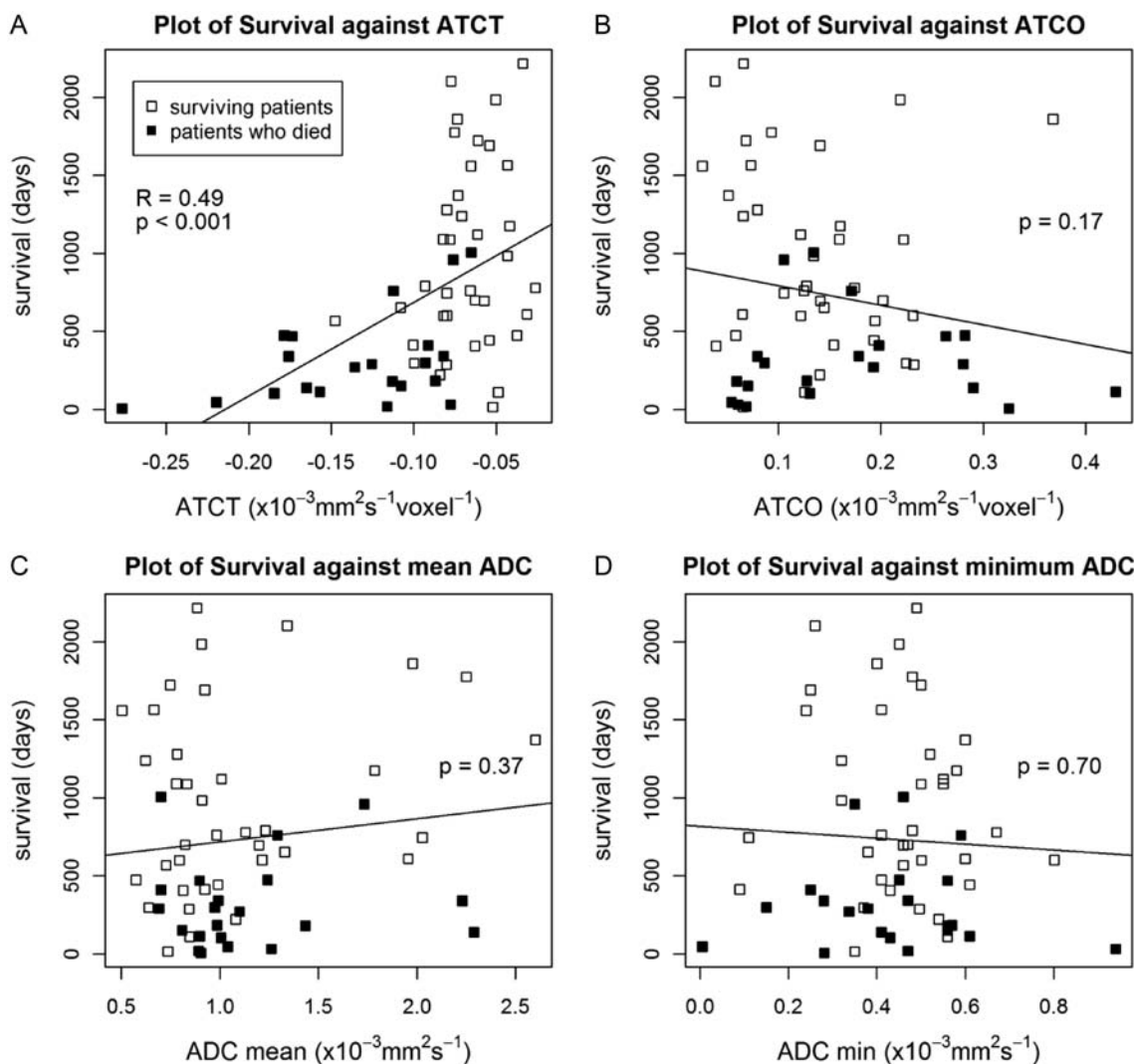
Fig. 2. Plot of survival against ATCT (A), ATCO (B), mean ADC (C), and minimum ADC (D) in 58 patients. Patients who died are marked by a black box and can be seen to have a more negative ATCT value in (A). A statistically significant linear fit to the data was observed for ATCT ($R = 0.49$, $P < .001$). No significant correlation between survival and ATCO, mean ADC, and minimum ADC was observed ($P = .17$, $P = .37$, and $P = .70$, respectively).

A linear correlation between survival and ATCO, mean ADC, and minimum ADC was not found to be statistically significant ($P = .17$, $P = .37$, and $P = .70$ respectively) (Fig. 2B–D).

Kaplan-Meier Curves

Kaplan-Meier curves showed a statistically significant survival benefit among children >3 years of age at diagnosis, compared with children <3 years of age at diagnosis ($P < .001$) (Fig. 3A) and among children who had total surgical resection ($P = .04$) (Fig. 3B). There was a trend for a difference in survival between ATRT, sPNET, and medulloblastoma (Fig. 3C), with the poorest survival in ATRT, followed by sPNET and medulloblastoma, but this did not reach statistical significance ($P = .09$). Patients with metastasis at presentation appeared to have a poorer survival outcome; however,

this was not found to be statistically significant ($P = .59$) (Fig. 3D).

Multivariate Survival Analysis

The Cox proportional hazard regression model indicated that the only statistically significant covariate was ATCT ($P < .001$). Age <3 years at diagnosis and extent of surgical resection were not found to be statistically significant covariates for the analysis ($P = .17$ and $P = .62$ respectively).

ATCT Kaplan-Meier Curves

ATCT was the only covariate yielding high statistical significance, and survival analysis using Kaplan-Meier curves was conducted by dividing the patients into 4 groups of equal size and increasing values of ATCT.
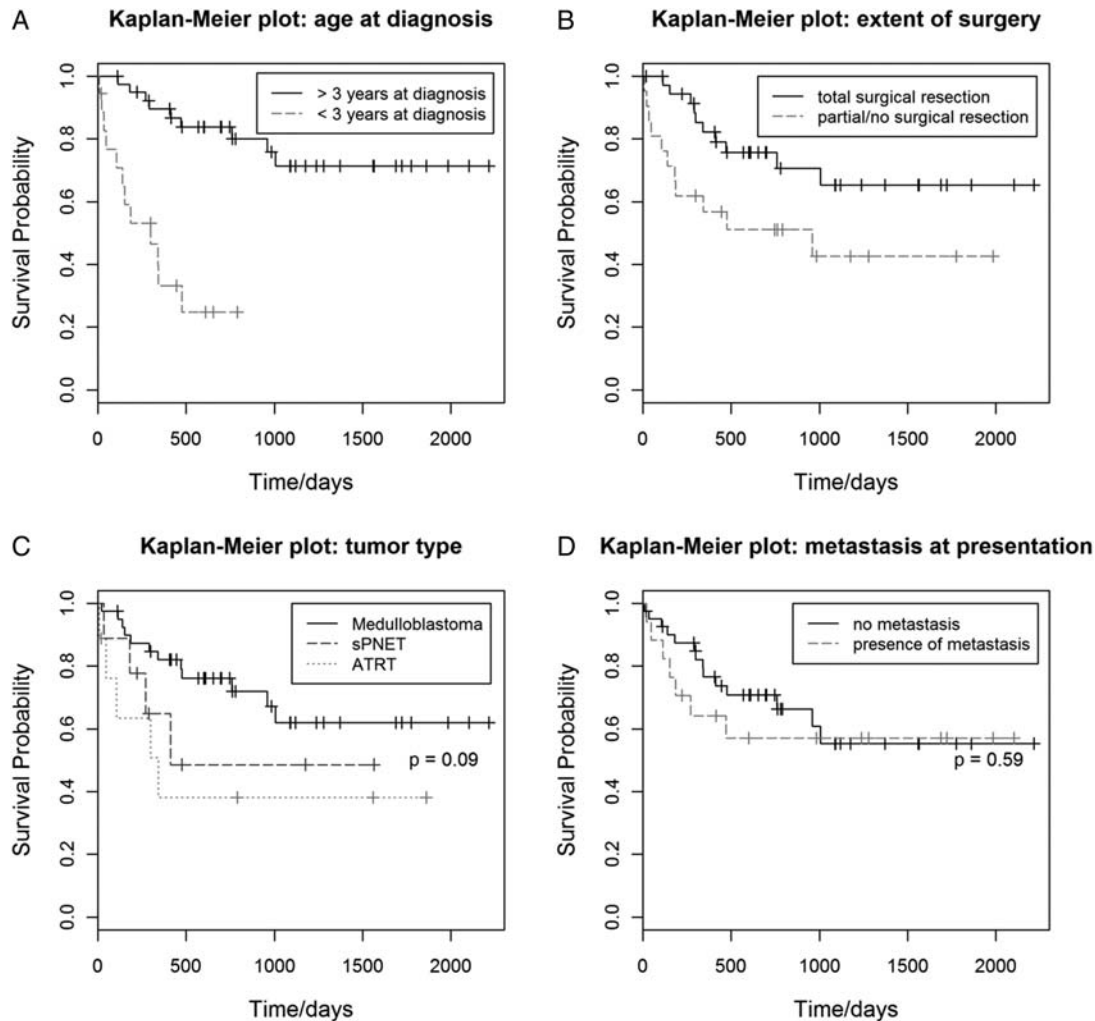
Fig. 3. Kaplan-Meier survival curves for age at diagnosis (A), extent of surgery (B), tumor type (C), and metastasis at presentation (D). Children <3 years of age are known to have a poorer prognosis, as confirmed by the survival curves, and a statistically significant $P < .001$. Children having had total surgical resection have a statistically significant higher chance of survival ($P = .04$). Tumor type and metastasis at presentation were not found to be statistically significant ($P = .09$ and $P = .59$, respectively).

The result showed that more negative values of ATCT were related to a lower chance of survival ($P < .001$). Kaplan-Meier curves show how survival differs in children with embryonal brain tumors as the value in ATCT changes (Fig. 4). Table 1 shows details of the survival outcome for the 4 different ATCT groups together with the median survival and the 25th centile. Lower values of median survival and 25th centile indicate a lower chance of survival and were identified in the groups with more negative ATCT values. Median survival and the 25th centile could not be measured in the less negative ATCT groups, because the survival probability was >50% and >75%, respectively, for the duration of the study.

Reproducibility Study

Bland-Altman analysis gives an indication of the variability between 2 measurements by plotting the difference between 2 repeated measurements against the mean of those 2 measurements. The CRs for the

intra- and interobserver analysis were found to be 0.0289 and 0.0238×10^{-3} mm^2 s^{-1} vox^{-1}, respectively, and the COVs were found to be 30.1% and 28.4%, respectively. In terms of the grouping in ATCT used in building the ATCT Kaplan-Meier survival curves, 7 of 10 patients and 8 of 10 patients remained in the same group for the intra- and the interobserver analysis, respectively. Of those patients changing groups, 4 were to an adjacent group and 1 was a change of 2 groups, whereas both patients who died stayed within the 2 most negative groups and both surviving patients moved to the least negative group. Overall, all patients who died fell in the 2 most negative groups, and the ones who survived fell within the 2 least negative groups for both the intra- and the interobserver analyses.

Discussion

The main finding of this study is that a statistically significant difference was observed for survival data in

children with embryonal brain tumors with respect to the change in ADC from peri-tumoral edema into the tumor volume. Our results show that more negative ATCT values are significantly associated with a poorer survival among children with embryonal brain tumors irrespective of tumor type, extent of resection, age <3 years at diagnosis, and metastasis at presentation. To our knowledge, no previous survival analysis has been published on the ATCT as a biomarker in children with embryonal brain tumors.

We hypothesize that an increased gradient change in ADC at tumor boundaries is related to a more malignant histological tumor type, thus explaining the lower survival outcome identified in our study.

ATCT

ADC has been shown to correlate with tumor cellularity in various tumor types. One study has shown a significant correlation between ADC values and tumor cellularity in medulloblastoma.[25] We believe that ATCT
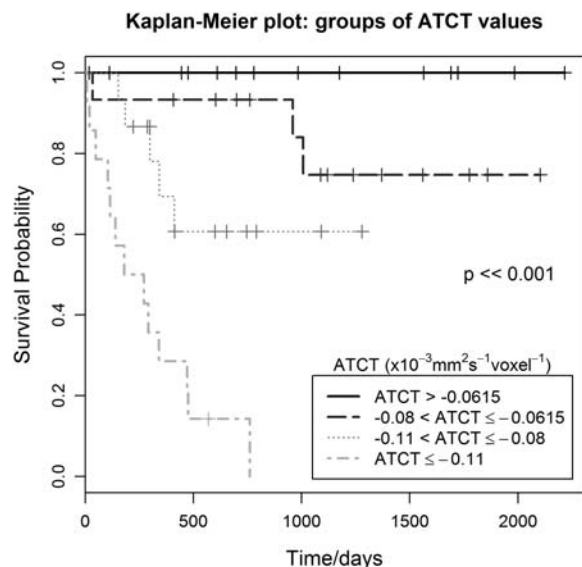

Fig. 4. Kaplan–Meier survival curves for increasingly negative values of ATCT show a decreasing survival probability ($P < .001$).

and, thus, the change in ADC over the edema-tumor boundary could be an indication of how rapidly the tumor cellularity is increasing (Fig. 5A and D) and that a more rapid increase in tumor cellularity from the edema-tumor boundary into the tumor is an indication of a poorer prognosis and reduced survival. More negative ATCT values could also be attributable to higher ADC values in the edema, indicating that cellularity might not be the only cause for poorer prognosis (Fig 5B and C). Previous studies focused on tumor border MRI features, and histology have shown that a sharper border on T_1- and T_2-weighted imaging could be indicative of an intact 1p/19q genotype, which is related to reduced survival in oligodendroglial tumors.[26,27] The results reported here support our hypothesis that tumor border biomarkers are useful indicators of survival in childhood embryonal brain tumors.

ATCO and Mean and Minimum ADC

The change in ADC from white matter into edema, the ATCO, was not found to correlate with survival. This result is consistent with previous findings showing that ATCO was not a good biomarker for survival outcome in adults with the highly malignant tumor glioblastoma multiforme.[14] Furthermore, in our cohort, mean ADC and minimum ADC values did not correlate with survival.

Tumor Type

Previous studies have shown that patients with sPNET have a poorer prognosis than do patients with medulloblastoma,[28] and patients with ATRT have a poorer prognosis than do patients with either medulloblastoma or sPNET[29]. To our knowledge, Kaplan–Meier survival analysis has not been published showing the difference in survival among these 3 embryonal brain tumors. In our analysis, these differences did not reach statistical significance; however, the observed trends in our data (Fig. 3C) are in line with current literature showing that patients with ATRT have the poorest prognosis and that patients with medulloblastoma have the best prognosis. The lack of statistical significance is likely to be attributable to the small number of patients with sPNET and ATRT in our cohort, reflecting the rarity

Table 1. Survival details for increasingly negative values of ATCT

ATCT range ($\times 10^{-3}$ mm^{2}s^{-1} vox^{-1})	$-(0-0.0615)$ Least negative	$-(0.0615-0.08)$	$-(0.08-0.11)$	$-(0.11-0.3)$ Most negative	Overall
No. of deaths/no. of patients	0/14	3/15	5/15	13/14	21/58
Median survival (days)	N/A	N/A	N/A	226	N/A
25th centile (days)	N/A	1006	342	104	299
<3 years (deaths/total)	0/3	1/1	4/7	7/7	12/18
Partial/no resection (deaths/total)	0/4	2/4	2/6	7/7	11/21

The table shows an increased number of deaths for more negative values of ATCT. The median survival gives the probable number of days 50% of the patients would survive in each group. The 25th centile gives the probable number of days 75% of the patients would survive in each group. Median survival and the 25th centile could not be measured in the less negative ATCT groups as the survival probability was higher than 50% and 75% respectively, for the duration of the study. Likelihood of survival is higher in the patients having less negative ATCT values.
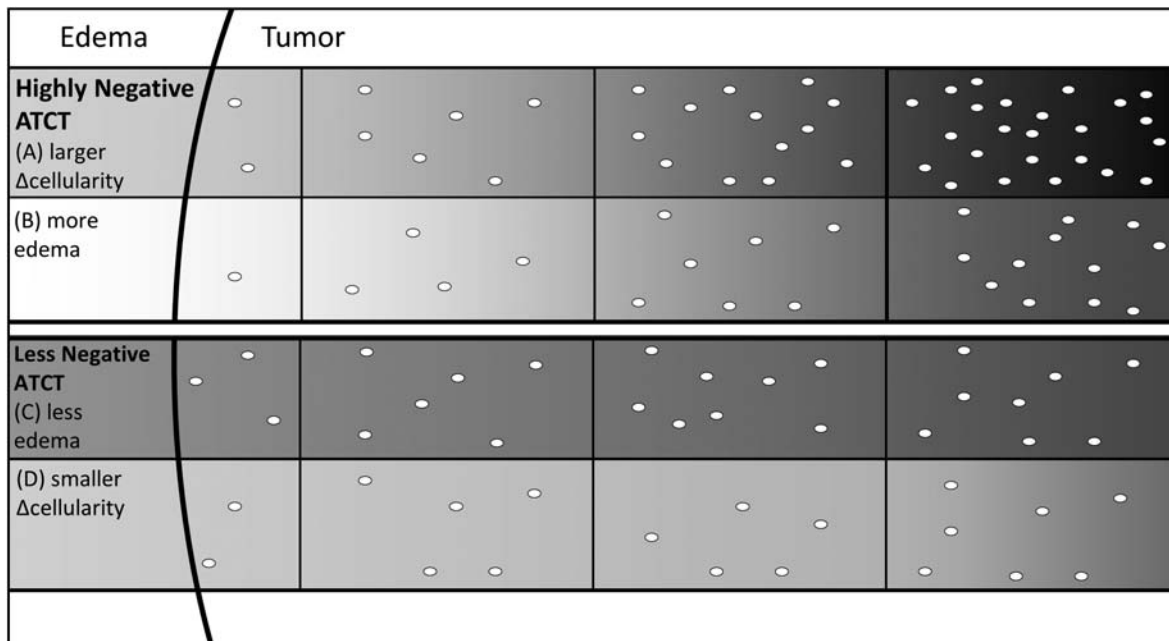
Fig. 5. Visualizing the ATCT. The image visualizes the hypothetical difference between a highly negative value of ATCT (A and B) and a less negative value of ATCT (C and D). A highly negative value of ATCT means that there is an increased change in ADC from the first voxel on the edema-tumor boundary toward the tumor core. We believe this is related to either a larger change in cellularity from the first voxel toward the tumor core (A) or due to increased edema in the first voxel (B). The increasingly darker shades of grey represent the decreasing values of ADC as tumor cellularity inside the corresponding voxel increases. Conversely, the less negative value of ATCT could be due to less edema being present (C) or due to a smaller change in cellularity from the first voxel towards the tumor core (D).

of these tumor types. However, when comparing pairs of tumor types, medulloblastoma was found to have statistically significant better survival than ATRT ($P = .04$), in agreement with previous literature,[29] whereas the trend for sPNETs to fare worse than medulloblastoma did not reach statistical significance ($P = .22$).

Metastasis at Presentation

Metastatic medulloblastoma[30] and metastatic ATRT[31] are well recognized to have reduced survival, compared with their nonmetastatic counterparts. Conflicting results have been obtained in patients with sPNET, with some studies finding no correlation between survival and metastasis at presentation.[32] In our results, we did not find a statistically significant difference in survival among patients with metastasis at presentation across the 3 tumor types. However, a trend for a poorer prognosis for those patients with metastasis can be seen in Fig. 3D. Again, the lack of statistical significance is likely to be attributable to the smaller sample size in this cohort, compared with the previous studies mentioned, which showed a difference in survival between patients with and without metastasis at presentation (119 patients in the study on medulloblastoma[30] and 48 patients in the study on ATRT[31]).

ATCT Across Embryonal Brain Tumors

The sample of tumors in our cohort included medulloblastoma, sPNET, and ATRT. We have recently shown

that parameters derived from ADC histogram measures can discriminate between ATRT and both sPNET and medulloblastoma.[33] It is important to establish that the ATCT can be applied generally across different types of embryonal tumors, broadening its clinical utility. However, we also examined correlation between ATCT and survival in the medulloblastoma group alone, and we found, similarly to the findings in the entire cohort, that ATCT was strongly correlated with survival in the medulloblastoma group ($P < .001$). We considered that the relatively small sample sizes in the sPNET and ATRT groups precluded a meaningful correlation of ATCT and survival in those groups if studied separately.

When looking at the survival analysis for the 3 embryonal tumor types, our findings, taken together, demonstrated that the ATCT is a more sensitive biomarker of survival than are age at diagnosis <3 years, extent of surgery, tumor type, and metastasis at presentation. The tumor types included in this sample reflect the typical presentation of embryonal tumors, such that the ATCT can be generalized across these tumor types.

Statistical Analysis

In our method, we described how a maximum of 3 covariates could be included in the multivariate analysis to retain sufficient statistical power. All variables were initially tested in a univariate analysis. Three covariates were found to be significant in the univariate analysis, and all of these were included in the multivariate

analysis. Therefore, there was no reason for including more covariates even if the method and numbers allowed us to do so.

Furthermore, in conducting Kaplan-Meier survival analysis and to visualize our findings, ATCT was categorized into groups. Having ATCT divided into 4 equal groups provided for an analysis with 3 different cutoff points, and as can be seen in the Kaplan-Meier curves, there does not appear to be a single cutoff point that determines favorable or unfavorable survival outcome. Results show that the more negative the cutoff point used, the worse the survival probability for each of the 3 cutoff points.

Study Limitations

This study is limited by various factors. ATCT is a subjective measurement, because edema and tumor boundaries are identified by visual inspection, and a maximum of 4 locations on the tumor borders were used in the calculation of the ATCT. This limitation is reflected in the reproducibility of the method. Semi-automated methods for voxel selection for the ATCT may improve the robustness of the method and could be a fruitful avenue for future work. Because the data were collected over a period of 7 years, some patients would have received different treatment regimes, with palliative care being offered in 5 cases. These different treatment procedures might have also had an impact on the survival outcome in this cohort.

Although the intra- and interobserver COVs for the ATCT were found to be 30.1% and 28.4%, respectively, the changes had a negligible impact on the overall results. The tendency for patients who died to fall in the 2 most negative groups and for the surviving patients to fall in the 2 least negative groups was maintained in all 10 cases analyzed for both the intra- and the interobserver analysis.

Medulloblastomas are classfied into 4 different histological subgroups (medulloblastoma with extensive nodularity, desmoplastic/nodular, anaplastic, and large cell medulloblastoma),[3] and recent advances in molecular genetics have indicated that medulloblastomas can be further classified into 4 different molecular subgroups (Wnt, Shh, group 3, and group 4).[34] However, in our center, these histological and molecular classifications have only been collected very recently and are not available for the majority of our cohort. Nonetheless, future studies could examine the ATCT in these distinct histological and molecular tumor types to evaluate the value of the ATCT as a biomarker in comparison with the predictive value of these classifications on survival.

Conclusion

In conclusion, identifying noninvasive biomarkers of survival outcome is of utmost importance in managing and planning the treatment of children with brain tumors. Our results show that ATCT, measured at diagnosis, is a sensitive biomarker that correlates with survival in childhood embryonal brain tumors.

Acknowledgments

Funding

References

1. Chawla A, Emmanuel JV, Seow WT, et al. Paediatric PNET: pre-surgical MRI features. *Clinical Radiology*. 2007;62(1):43–52.

2. Klisch J, Husstedt H, Hennings S, et al. Supratentorial primitive neuroectodermal tumours: diffusion-weighted MRI. *Neuroradiology*. 2000;42(6):393–398.

3. Louis D, Ohgaki H, Wiestler O, et al. The 2007 WHO classification of tumours of the central nervous system. *Acta Neuropathol*. 2007;114(2):97–109.

4. Newton HB, Ray-Chaudhury A, Malkin MG. Overview of pathology and treatment of primary brain tumours. In: Newton, HB, Jolesz, FA, ed. Handbook of Neuro-Oncology Neuroimaging. Amsterdam: Academic Press; 2008:9–19.

5. Chenevert TL, Stegman LD, Taylor JM, et al. Diffusion magnetic resonance imaging: an early surrogate marker of therapeutic efficacy in brain tumors. *Journal of the National Cancer Institute*. 2000;92(24):2029–2036.

6. Ellingson BM, Malkin MG, Rand SD, et al. Validation of functional diffusion maps (fDMs) as a biomarker for human glioma cellularity. *J Magn Reson Imaging*. 2010;31(3):538–548.

7. Gauvain KM, McKinstry RC, Mukherjee P, et al. Evaluating pediatric brain tumor cellularity with diffusion-tensor imaging. *AJR*. 2001;177(2):449–454.

8. Sugahara T, Korogi Y, Kochi M, et al. Usefulness of diffusion-weighted MRI with echo-planar technique in the evaluation of cellularity in gliomas. *J Magn Reson Imaging*. 1999;9(1):53–60.

9. Kotsenas AL, Roth TC, Manness WK, Faerber EN. Abnormal diffusion-weighted MRI in medulloblastoma: does it reflect small cell histology? *Pediatric Radiology*. 1999;29(7):524–526.

10. Matsumoto Y, Kuroda M, Matsuya R, et al. In vitro experimental study of the relationship between the apparent diffusion coefficient and changes in cellularity and cell morphology. *Oncology Reports*. 2009;22(3):641–648.

11. Padhani AR, Liu G, Koh DM, et al. Diffusion-weighted magnetic resonance imaging as a cancer biomarker: consensus and recommendations. *Neoplasia*. 2009;11(2):102–125.

12. Aghi M, Gaviani P, Henson JW, et al. Magnetic Resonance Imaging Characteristics Predict Epidermal Growth Factor Receptor Amplification Status in Glioblastoma. *Clinical Cancer Research*. 2005;11(24):8600–8605.

13. Jenkinson MD, Smith TS, Brodbelt AR, et al. Apparent diffusion coefficients in oligodendroglial tumors characterized by genotype. *J Magn Reson Imaging*. 2007;26(6):1405–1412.

14. Thompson G, Cain JR, Mills SJ, Jackson A. Apparent Diffusion Coefficient Measures on MR Correlate with Survival in Glioblastoma Multiforme [abstract]. *Proc Intl Soc Mag Reson Med*. 2009;17:280.

15. Razek AAKA, Megahed AS, Denewer A, et al. Role of diffusion-weighted magnetic resonance imaging in differentiation between the viable and necrotic parts of head and neck tumors. *Acta Radiologica*. 2008;49(3):364–370.

16. Vossen JA, Buijs M, Geschwind JFH, et al. Diffusion-Weighted and Gd-EOB-DTPA–Contrast-Enhanced Magnetic Resonance Imaging for Characterization of Tumor Necrosis in an Animal Model. *J Comput Assist Tomogr*. 2009;33(4):626.

17. Clark TG, Bradburn MJ, Love SB, Altman DG. Survival Analysis Part I: Basic concepts and first analyses. *Br J Cancer*. 2003;89(2):232–238.

18. Bradburn MJ, Clark TG, Love SB, Altman DG. Survival Analysis Part II: Multivariate data analysis - an introduction to concepts and methods. *Br J Cancer*. 2003;89(3):431–436.

19. Bradburn MJ, Clark TG, Love SB, Altman DG. Survival Analysis Part III: Multivariate data analysis - choosing a model and assessing its adequacy and fit. *Br J Cancer*. 2003;89(4):605–611.

20. Clark TG, Bradburn MJ, Love SB, Altman DG. Survival Analysis Part IV: Further concepts and methods in survival analysis. *Br J Cancer*. 2003;89(5):781–786.

21. R Core Team (2012). R: A language and environment for statistical computing. R Foundation for Statistical Computing, Vienna, Austria. ISBN 3-900051-07-0. Available at: http://www.R-project.org/.

22. Therneau T. Survival: Survival analysis, including penalised likelihood. 2010. Available at: http://cran.r-project.org/web/packages/survival/index.html.

23. Bland JM, Altman DG. Statistical methods for assessing agreement between two methods of clinical measurement. *The Lancet*. 1986;1(8476):307–310.

24. Bland JM, Altman DG. Measuring agreement in method comparison studies. *Statistical Methods in Medical Research*. 1999;8(2):135–160.

25. Yamashita Y, Kumabe T, Higano S, Watanabe M, Tominaga T. Minimum apparent diffusion coefficient is significantly correlated with cellularity in medulloblastomas. *Neurological Research*. 2009;31(9):940–946.

26. Jenkinson MD, du Plessis DG, Smith TS, et al. Histological growth patterns and genotype in oligodendroglial tumours: correlation with MRI features. *Brain*. 2006;129(7):1884–1891.

27. Megyesi JF, Kachur E, Lee DH, et al. Imaging correlates of molecular signatures in oligodendrogliomas. *Clinical Cancer Research*. 2004;10(13):4303–4306.

28. Packer RJ, Macdonald T, Vezina G, Keating R, Santi M. Medulloblastoma and primitive neuroectodermal tumors. *Handbook of Clinical Neurology*. 2012;105:529–548.

29. Ho DM, Hsu CY, Wong TT, Ting LT, Chiang H. Atypical teratoid/rhabdoid tumor of the central nervous system: a comparative study with primitive neuroectodermal tumor/medulloblastoma. *Acta Neuropathologica*. 2000;99(5):482–488.

30. Ray A, Ho M, Ma J, et al. A clinicobiological model predicting survival in medulloblastoma. *Clinical Cancer Research*. 2004;10(22):7613–7620.

31. Dufour C, Beaugrand A, Le Deley MC, et al. Clinicopathologic prognostic factors in childhood atypical teratoid and rhabdoid tumor of the central nervous system: A multicenter study. *Cancer*. 2012:118(15):3812–3821.

32. Johnston DL, Keene DL, Lafay-Cousin L, et al. Supratentorial primitive neuroectodermal tumors: a Canadian pediatric brain tumor consortium report. *Journal of Neuro-Oncology*. 2008;86(1):101–108.

33. Bull JG, Saunders DE, Clark CA. Discrimination of paediatric brain tumours using apparent diffusion coefficient histograms. *European radiology*. 2012;22(2):447–57.

34. Northcott PA, Korshunov A, Witt H, et al. Medulloblastoma comprises four distinct molecular variants. *J Clin Oncol*. 2011;29(11):1408–1414.